Methods for Determining the Primary Energy of Cosmic Ray Showers

J. Cortina[1], F. Arqueros[1], E. Lorenz[2]

[1] Departamento de Fisica Atomica, Molecular y Nuclear, Facultad de Ciencias Fisicas, Universidad Complutense, 28040 Madrid, Spain.
[2] Max-Planck Institut für Kernphysik, Fohringer Ring 6, 80805 München, Germany.

Abstract. Monte Carlo simulations of cosmic ray induced showers in the atmosphere have been used to develop three new methods for measuring the energy of the primary particles in the 10^{13} - 10^{16} eV range independently of the particle species. Both the electron number and the Cherenkov light density near and beyond the hump in the lateral distributions are found to accurately indicate the primary energy, provided an appropriate correction based on the depth of the shower maximum is applied. The depth of shower maximum can be estimated from the slope of the radial distribution of the Cherenkov light. In addition, simultaneous measurement of the muon number and the Cherenkov light intensity also provides a very accurate measure of the primary energy. All of these parameters can be determined using existing particle detector arrays. A very precise measurement of the cosmic ray all-particle spectrum regardless of chemical composition is thus shown to be practicable.

1 Introduction

The study of the cosmic ray energy spectrum in the 10^{13} - 10^{16} eV range is of the utmost relevance to the continuing quest for the origin of these particles. The sudden change in the spectral slope which takes place at about 3×10^{15} eV (the so-called *knee*, [1, 2]) is particularly significant. It is still unclear as to whether the *knee* is caused by the magnetic confinement of cosmic rays in our galaxy or is due to some feature of the cosmic ray sources themselves (see [2] for a review of both scenarios). Measurements in this energy range are still not precise enough, indeed the exact location of the *knee* is still unclear. Our knowledge of the spectral features relies on our ability to accurately determine cosmic ray energies. Primary energies can be directly measured using satellite-borne detectors below a few PeV. For higher energies indirect methods based on the detection of the Extensive Air Shower (EAS) at ground level are required. In this case primary energy is usually inferred from the number of electrons N_e and/or the number of muons N_μ in the shower, which are both measured with particle counter arrays. Several contemporary arrays provide the capability to measure the spectrum in a wide energy interval around the *knee* by means of this technique [3, 4, 5].

The relationship between the particle number N_e or N_μ and the primary energy E_0 depends critically on the mass number of the primary nucleus, i.e., the chemical composition. Unfortunately, the chemical composition in this energy range is still largely unknown [6]. In fact, even if the species of the primary particle were known, the accuracy in the energy measurement of individual showers would be limited by the strong fluctuations in the shower's longitudinal development.

High energy particles of an air shower generate Cherenkov radiation which is strongly forward peaked and thus can be detected at ground. Cherenkov light contains information about the shower development. Due to the low and variable density of the atmosphere, Cherenkov radiation is not exactly proportional to the ionisation loss of the charged particles, therefore the combination of the atmosphere and a distributed light detector forms a fully active but "non-compensating" calorimeter. This calorimetric feature provides a better measure of the primary energy than that based on the number of particles at ground. In fact wide-angle detection of the Cherenkov light at ground level has long been used to measure E_0 [7]. Particularly the HEGRA AIROBICC array [3], consisting of 77 open photomultiplier tubes viewing the night sky over a solid angle of about 1 steradian, makes efficient use of this principle [8]. In addition it has already shown an outstanding capability to accurately record features of the lateral distribution of EAS Cherenkov light in the energy range of interest here. In particular, the Cherenkov light density can be determined with an uncertainty ranging from just 5 to 10%.

We will show in this paper that a species-independent measurement of the primary energy is possible using either the number of electrons or the Cherenkov light on condition that an appropriate correction, depending on the position of the shower maximum, is applied (for a similar method, see [9]). As is well known, the Cherenkov light lateral distribution provides a measure of the shower maximum position [10] (see section 3). Therefore either a combined detector consisting of a Cherenkov array plus an electron-counter array or a Cherenkov counter array working in stand-alone mode is able to provide a measure of E_0 which is independent of the primary nucleus type. A precise and composition independent energy measurement is equally important for experiments which try to reveal the chemical composition.

These arrays are also being used in the search for point sources of photons of 10^{13} - 10^{16} eV [11]. No convincing detection has been reported so far, because the achieved sensitivity is barely sufficient to observe the strongest sources seen at lower energies, provided the spectra continue according to the measured power laws. In the event of a positive detection, an exact energy measurement of the primary γ-rays would be extremely valuable to theorists. We will show that the methods developed in this paper can be applied to measure the primary energy of pure electromagnetic showers with great accuracy.

This study relies on a Monte Carlo (MC) simulation of shower development which has been carried out using the CORSIKA code [13]. The results presented in section 4 do not take into account any detector features and thus represent a theoretical limit to the expected accuracy of the E_0 measurement. Nonetheless, a detailed simulation of the HEGRA array performance [12] shows that, in practice, our method provides an energy measure with an accuracy significantly better than that achieved to date for both hadronic and γ-ray primaries in this energy range.

2 Monte Carlo simulation

Showers have been simulated using the CORSIKA code (version 4.068). This code was developed by members of the KASKADE collaboration [5]. CORSIKA allows users to choose among several models for the simulation of both the electromagnetic (EM) and the hadronic components. In this work, the EM component was simulated using the well-known EGS4 code [14]. The chosen cutoff energy for secondary γ-rays and electrons was 3 MeV. Hadronic interactions with energy in the laboratory system lower than 80 GeV were treated with the GHEISHA code [15] while, at higher energies, the VENUS (version 4.12, [16]) and HDPM [13] codes were employed for $Z>1$ and $Z=1$ respectively. VENUS is based on the Gribov-Regge theory and describes soft particle interactions by the exchange of pomerons. HDPM extrapolates experimental data from low to high energies and from high to low transverse momenta. Nuclei are considered as superpositions of free nucleons (a comparison of these two models and some others in extensive use in EAS calculations can be found in [17]). The kinetic energy cut for hadrons and muons was set to 10 MeV.

Data on the electron-photon component and the Cherenkov radiation at ground level were stored for each individual shower. The observation level was set to an atmospheric depth of about 800 g/cm^2 which corresponds to the altitude of the Roque de los Muchachos Observatory where the HEGRA experiment is installed.

The primary species considered in this work included hydrogen, oxygen and iron nuclei as well as γ-rays, with primary energies ranging from 10 TeV to 10 PeV. As zenith angle we have chosen 10 or 25 degrees. The number of simulated events per primary particle per angle of incidence was approximately 1000. These showers were generated with a power law spectrum of spectral index -1. In addition, a sample of 400 showers with 100 TeV primary energy was simulated from which we studied in detail the shower features at a fixed energy.

An accurate simulation of the electron-photon component is extremely time consuming at energies above 1 PeV. In order to operate in such an extreme range, CORSIKA makes use of some laboursaving approximations. Firstly, Cherenkov photons are grouped into bunches, each of which is subsequently treated as a single photon in calculating the impact point at ground level [12]. Secondly, the step size between consecutive applications of the multiple scattering formulae, which simulate the electron trajectories, is significantly larger than that suggested by EGS4. Whilst bunching is expected to have a negligible effect upon the radial distribution of the Cherenkov light, the enlargement of the multiple scattering step size can have some effect on it. The simulation generates radial distributions of Cherenkov light in the 300-500 nm wavelength interval. Atmospheric attenuation has not been taken into account. However, the physical basis of the primary energy determination methods shown in this paper should not be affected by these systematic errors. In fact the methods shown in this paper are already being applied in the HEGRA experiment. A shower library which includes the appropiate scattering step size and atmospheric attenuation, as well as a detailed simulation of both the HEGRA scintillator array and the Cherenkov counter array (AIROBICC) is in preparation [18]. Preliminary results show that the methods presented here are valid.

3 Depth of the shower maximum

The relationship between the longitudinal development of an extensive air shower and the features of the Cherenkov radiation at ground level has been extensively discussed in [19]. We review in this section some facts which are relevant to our methods.

The most relevant feature of the longitudinal development is the altitude at which the maximum development of the shower takes place. Alternately, the shower maximum depth X_{max} (i.e. the air mass overburden per unit area at the position of the shower maximum) is commonly used. Figure 1 shows the dependence of X_{max} on E_0 for hydrogen, oxygen and iron nuclei in the energy range under study. X_{max} increases with the primary energy, while, conversely, for a fixed E_0, X_{max} decreases with the mass number of the primary nucleus A, since the heavier the primary is, the higher in the atmosphere the first interaction takes place. From this figure it can also be inferred that the relationship between X_{max} and E_0/A is only weakly dependent upon the primary nucleus. In nucleus initiated showers, the hadronic core continuously feeds the EM component of the cascade, therefore these showers are of greater longitudinal extent than those initiated by γ-rays.

In hadron initiated showers the number of interaction generations before the shower maximum increases with $\log(E_0)$. In each generation, about one third of the total energy is transformed into neutral pions. As a consequence, assuming that the shower maximum is well above the observation level, the fraction of the primary energy which is transferred to the EM component, f_{em}, is expected to increase linearly with $\log(E_0)$ (see figure 2 and [20]). In fact, as shown in figure 2b, f_{em} depends on the primary energy per nucleon, as expected from the superposition model.

Since both X_{max} and f_{em} depend linearly on $\log(E_0/A)$ in this energy range, X_{max} is expected to depend linearly on f_{em}, as can be seen in figure 3 for showers of 10 degrees zenith angle. The above arguments do not hold if the shower maximum is not well above the observation level, since very deep showers are absorbed at ground before full development. In figure 3, it appears that, for very deeply interacting proton showers, f_{em} is smaller than expected from a linear dependence. We have checked that this f_{em} "saturation" is, as expected, less significant for 25 degree showers, since X_{max} at a given energy decreases with zenith angle. The relationship between X_{max} and f_{em} shown in figure 3 is a consequence of the dependence of both parameters on E_0. In fact we have checked that, as expected, fluctuations of X_{max} and f_{em} are uncorrelated for a fixed E_0 value.

The energy transferred to the EM component of the shower $E_{em} = f_{em} \times E_0$ is invested in the creation of electrons (and positrons). These are the main contributors to the generation of Cherenkov light because of their large numbers and lower Cherenkov energy threshold as compared to other charged shower particles. The shape of the lateral distribution of Cherenkov light at ground is well known [19]. Near the shower axis the light density ρ decreases with the core distance r, following an exponential law:

$$\rho(r) = a \ \exp(-r/r_L) \tag{1}$$

where r_L, the so-called "light radius", provides a measure of X_{max}. At a radial distance of about 120 m (this value slightly depends on the observation altitude and zenith angle), a change in the slope of $\rho(r)$ takes place (this constitutes the "hump" in the Cherenkov lateral distribution) which is particularly prominent for γ-ray showers below 100 TeV.

In figure 4 we show X_{max} versus log r_L for showers of 10 degree zenith angle following our MC predictions. The values of the r_L parameter have been obtained by means of a fit of the simulated light density in the radial interval 10 - 100 m to function 1. As can be seen in this figure the relationship between X_{max} and $\log(r_L)$ is nearly the same for all primary nuclei. Note that X_{max} decreases with the zenith angle; essentially it depends on the atmospheric mass between the position of the shower maximum and the observer. The experimental determination of r_L, which can be carried out using an array of Cherenkov light counters, allows one to measure X_{max} for individual showers. Uncertainties in such a determination come from both intrinsic fluctuations of the shower longitudinal development and detector limitations (e.g. sampling effects, uncertainty in the core location, etc..). According to our MC results, the expected uncertainties due to intrinsic fluctuations range from 40 g/cm^2 (70 g/cm^2) for protons (iron nuclei) in the energy range 50 - 100 TeV to less than 25 g/cm^2 for all nuclei at E_0 >1 PeV. For showers initiated by γ-rays the expected uncertainties are even less (30 g/cm^2 in the range 50 - 100 TeV and 15 g/cm^2 at E_0 >1 PeV) because of the smaller fluctuations in pure EM showers.

A detailed detector simulation [18] shows that these errors are not expected to increase significantly in a real experiment. Any discrepancies do not exceed the statistical fluctuations given the limited number of simulated events.

4 Primary energy

As noted in the introduction, one of the traditional methods of determining the primary energy of a cosmic ray shower is based on measurement of the number of electrons at ground level, N_e. This method enables one to measure the energy transferred to the EM channel. Unfortunately, N_e is sensitive to strong fluctuations in the longitudinal development of the shower (which basically depend on X_{max}).

The total amount of Cherenkov light at the observation level is also a measure of E_{em}, but in a calorimetric way. Therefore, measurement of the Cherenkov light leads to a better determination of the primary energy than does the measurement of N_e (below we show that the Cherenkov light density near or beyond the hump position is the better measure of E_{em}). This measurement is weakly related to the shape of the longitudinal development via the changing Cherenkov threshold and the different attenuation suffered by Cherenkov photons emitted at different heights (both factors being basically dependent on X_{max}).

Measurement of f_{em} is necessary to convert E_{em} into E_0. As discussed in section 3, f_{em} strongly depends on primary type. As already mentioned, X_{max} (which can be determined from the slope of the radial distribution of the Cherenkov light as shown in figure 4) provides a primary independent measure of f_{em}, because both parameters depend in a similar way on E_0/A. Fluctuations of f_{em} for a fixed primary energy limit the accuracy of our E_0 measurement method (sections 4.1 and 4.2).

An additional method of estimating f_{em} is to measure the number of muons in the shower, which is related to the fraction of the primary energy not transferred to the EM channel. This measurement bypasses both fluctuations in f_{em} and dependence on primary type. In practice, this can only be achieved at high enough energies. In section 4.3, a method is introduced which combines information from Cherenkov light and N_μ.

As previously mentioned, the measurement of the primary energy of γ-ray showers in the energy range of this work is of great importance in the search for sources of ultra-high energy photons. The methods of energy measurement described below can also be applied to γ-ray initiated showers. Since for these f_{em}=1 (i.e. f_{em} does not fluctuate) a much better precision is expected for γ-ray showers than for those due to nuclei.

4.1 Energy Measure from N_e

Figure 5a shows shower size versus primary energy for showers initiated by γ-rays, protons and iron nuclei at 10 degree zenith angle. Symbols indicate the mean values of the N_e distribution whilst vertical error bars represent its (root mean square) fluctuations. This figure shows that the relationship between N_e and E_0 strongly depends on the primary type. The significant effect of statistical fluctuations can also be seen. While, for a pure EM shower, N_e fluctuations are only due to fluctuations in the EM cascade development, f_{em} fluctuations also play a significant role in hadronic showers. For heavy primaries like iron nuclei, fluctuations are less significant, as expected from the superposition model.

As is well known [12], the relationship between E_0 and N_e can be approximately described by:

$$E_0 = B \cdot N_e^b \tag{2}$$

where the parameters B and b depend on the primary particle. In addition, the parameter B depends on the angle of incidence of the primary particle, while in the first order b, which is very close to unity, does not. Assuming that we know the primary type (which is not usually the case), equation 2 provides a calibration function for the measurement of E_0. In fact, as can be seen in figure 5a, either a fit to a second order polynomial or a linear fit (as equation 2) dependent on the energy range provides a better measure of E_0. By comparing the real E_0 value (input parameter in the MC generator) with that determined from equation 2, the expected uncertainties in the value of the energy can be inferred. In this work, this uncertainty has been calculated as the root mean square of the distribution of the percentage differences between the real energy and that predicted by the calibration function. Table 1 shows the resulting uncertainties Δ_p, for several primary particles in three energy intervals E_0 <100 TeV, 100 TeV <E_0 < 500 TeV and E_0 > 500 TeV. As expected, Δ_p decreases with E_0 and for hadronic showers it also decreases with A. Table 1 also includes the values of Δ_p calculated for γ-ray showers up to an energy of 500 TeV.

In figure 6a, N_e is plotted versus X_{max} for a sample of showers initiated by various primary particles (γ-rays, protons and iron nuclei) of identical energy, in this case 100 TeV. As mentioned above, N_e grows with X_{max} for a given primary type, since the lower the shower maximum takes place in the atmosphere, the higher the number of electrons reaching observation level is. As can be seen from the figure the correlation is particularly strong for γ-ray showers. Henceforth, a knowledge of X_{max} allows accurate determination of E_{em} via measurement of N_e. Note that this figure shows that for a fixed E_0 value the average N_e value decreases with A for hadronic primaries, since f_{em} also decreases with A.

It follows that X_{max} can be applied either to correct N_e for fluctuations of shower development or to compensate for the dependence of f_{em} on the primary nucleus. As a matter of fact, an almost identical relationship N_e (X_{max}) enables one to simultaneously correct N_e for both effects. Similar behaviour has been observed throughout the energy range of this work. Taking into account the fact that the light radius of the lateral distribution of Cherenkov light is a measure of X_{max} it is therefore expected that a corrected number of electrons N_e^c given by

$$N_e^c = N_e \times (r_L/\mathrm{m})^\alpha \tag{3}$$

will provide a good measure of E_0, independent of the primary particle and also substantially corrected for fluctuations in the longitudinal development.

The free parameter α can be chosen to minimize the primary type bias in the determination of E_0 over the energy range of interest. Figure 5b shows the effect of the above correction for a value of α = 1.25, for which the function $E_0(N_e)$ is least dependent on the primary type at a zenith angle of 10 degrees. Since α depends on the slope of the $N_e(X_{max})$ function and both N_e and X_{max} vary with θ in differing ways, the optimal value of α is expected to vary according to the angle of incidence. In fact, α has been found to increase with θ, reaching a value of 1.75 at 25 degrees. The resulting N_e^c value provides, therefore, a primary independent measure of E_0. The corresponding uncertainties Δ_i^c have been calculated as before. The results are also shown in table 1. From this table it can be seen that in most cases Δ_i^c is lower than Δ_p, as expected, since the application of equation 3 also reduces the effect of the statistical fluctuations in the longitudinal development (see figure 5).

Alternatively, the α parameter of equation 3 can be chosen in order to minimize the energy error for each primary particle independently. This procedure leads to a very accurate measurement of E_0, although the calibration law is then dependent on the primary type. The corresponding energy uncertainties Δ_p^c, which are also given in table 1, are significantly smaller than Δ_p, as expected.

Unfortunately, such accuracy in the measurement of E_0 is only possible if the primary particle is known. As shown in table 1, the application of this procedure to γ-ray showers significantly improves the accuracy of the E_0 determination.

As previously mentioned, in calculating the uncertaintes in the measurement of E_0 shown here, we have not taken into account any detector effects. However, a detailed simulation of the scintillator array and of the Cherenkov counter array (AIROBICC) of the HEGRA experiment is underway [18]. Preliminary results suggest that the detector effect can be roughly taken into account, by adding in quadrature to the percentage errors shown in table 1 a value which ranges from about 30% in the lower energy range down to about 10% at the highest energies (see [18] for further details).

4.2 Energy measure from the Cherenkov light

As already suggested, a "calorimetric" measurement of the total amount of Cherenkov light should provide a very good determination of E_{em}. However, for a given E_{em} value, the amount of Cherenkov light at ground level is subject to non-negligible fluctuations. The energy threshold for Cherenkov emission varies with altitude (because of the changing air density) and the atmospheric attenuation of the Cherenkov light depends on the air mass traversed in reaching the observation level. Therefore, the total amount of Cherenkov light at the observation level depends on the features of the longitudinal development (in particular, the position of the shower maximum). In addition, most real detectors are not large enough to incompass the full light disc. The lateral distribution of the Cherenkov light depends on the longitudinal development of the shower and, therefore, the fraction of undetected light also depends on X_{max}. The conclusion is that the total amount of Cherenkov light is not the optimum parameter for the measurement of E_{em}.

It is well known [10] that the density of Cherenkov light around (and beyond) the hump position, ρ_{hump}, is only weakly dependent on the fluctuations in the shower development for γ-ray showers. As a consequence, ρ_{hump} is a good measure of the primary energy of a pure EM shower. ρ_{hump} is well correlated with E_{em} for hadronic showers, as shown in figure 7a, and therefore it provides a good measure of E_0, assuming that we know the primary nucleus [12].

In order to understand the origin of this effect, we have done the following. Applying a similar method to that previously used in [21] the atmosphere has been divided into layers. The ratio $R_l(r)$ of the number of Cherenkov photons generated in each layer which arrive at a core distance r to the total number of photons produced in the layer has been calculated. Figure 8 shows $R_l(r)$ for four layers for a γ-ray shower of 100 TeV. This figure illustrates that R_l is basically independent of the altitude around the hump and therefore ρ_{hump} is not expected to be very sensitive to fluctuations in the shower development. It should be noted that the main contribution to $\rho(r)$ comes from the layers near the shower maximum while the upper layers (e.g. that from 100 - 150 g/cm^2 in figure 8) contribute substantially less. At an energy of 100 TeV, the deepest layers (700 - 750 g/cm^2 in figure 8) also make a small contribution. This figure shows that the layers which produce the bulk of the Cherenkov light contribute very similar percentages at a core distance larger than 150 m. Therefore, the light density at r$>$ 150 m is also expected to provide a good indication of E_{em} for a hadronic shower. This can be seen in figure 7b where E_{em} has been plotted versus the light density at 200 m distance, ρ_{200}, for all primary nuclei across the entire energy range of this work. In fact ρ_{200} turns out to be a better measure of E_{em} than does ρ_{hump}, particularly at low primary energies. Unfortunately, the experimental measurement of the light density becomes very difficult beyond the hump position. Not only does it require a very extended array of Cherenkov light detectors, but the fluctuations of the night sky light become comparable to the Cherenkov light density at large core distances for primary energies below about 1 PeV.

Figure 9a shows ρ_{hump} versus E_0 for the showers of figure 5. The dependence of f_{em} on the primary nucleus is clearly visible in this figure. By comparing figures 5a and 9a it can be seen that, as expected, the ρ_{hump} fluctuations are significantly smaller than those of N_e.

The relationship between E_0 and ρ_{hump} can be described by:

$$E_0 = D \cdot \rho_{hump}^d \qquad (4)$$

where the parameters D and d are analogous to B and b of equation 2 respectively. Given equation 4, E_0 can be found from ρ_{hump} assuming that the primary particle is known. It can also be obtained from ρ_{200} in a similar fashion. Following the procedure described in section 4.1, the expected uncertainties in the determination of the energy from the light density at the hump, Δ_{hump}, have been calculated. The results are shown in table 2. When using ρ_{200} the energy uncertainties are found to be slightly smaller in the low energy range. Comparing these results with those in table 1, it is seen that ρ_{hump} provides a much better measure of the energy as compared to that obtained from N_e.

This method is particularly precise for the measurement of the primary energy of γ-ray showers, for which an uncertainty ranging from 9 to 5% is expected (see table 2).

A realistic simulation of the AIROBICC array of Cherenkov counters [18] shows that for hadronic showers, the detector effect can be roughly taken into account by adding quadratically to the percentage errors shown in table 2 a value which ranges from about 15% at the lower energy edge down to about 5% at the highest energies. This detector effect includes the smearing of the Cherenkov light signal, the uncertainty in the core position and the effect of the limited physical extent of the array.

In figure 6b ρ_{hump} is shown versus X_{max} for showers initiated by several primaries of 100 TeV energy. It can be clearly seen that fluctuations in ρ_{hump} are significantly smaller than those of N_e (see figure 6a). Therefore, a measurement of X_{max} is not expected to substantially improve our precision in determining E_{em} for each individual primary. For a given primary energy, the average f_{em} value depends on the primary type and therefore ρ_{hump} also depends on the primary nucleus. Since X_{max} provides a measure of the average f_{em} independently of the primary type, measurement of r_L can provide the information required to achieve a primary independent determination of the energy.

Following a procedure similar to that described in section 4.1, a corrected light density ρ^c_{hump} can be defined as:

$$\rho^c_{hump} = \rho_{hump} \times (r_L/\mathrm{m})^{\beta} \tag{5}$$

where the free parameter β is chosen in order to achieve a primary independent measurement of E_0. We have found that the optimal β values are approximately 0.75 and 1.0 for showers initiated by cosmic rays at 10 and 25 degree zenith angles respectively. In fact, a better energy determination can be achieved by using a β value which slightly depends on light density, in order to take into account small deviations from the expected behaviour across the whole energy range. In this work the empirical law $\beta(\rho_{hump})=\beta_0+\omega\times\log(\rho_{hump})$ has been used, where β_0 and ω are free parameters. Figure 9 shows that the function $\rho^c_{hump}(E_0)$ is independent of the primary nucleus. Unfortunately this correction enlarges the fluctuations, as expected given figure 6b. As a consequence, the uncertainties in this primary independent measure of the energy Δ^c_{hump} are significantly larger than Δ_{hump} (see table 2). This is the price of a primary independent measurement. Finally, table 2 shows the results of the application of this procedure using the light density at 200 m. The expected energy uncertainties Δ^c_{200} are smaller than Δ^c_{hump}, particularly in the low energy range, since ρ_{200} is better than ρ_{hump} as a measure of E_{em} and therefore the method is expected to be more effective when the light density beyond the hump position is used.

The effect of a real detector is to add in quadrature to Δ^c_{hump} and Δ^c_{200} values ranging from about 50% at the lowest energies in this study down to about 15% at the highest [18].

4.3 Energy measure from the number of muons

Whilst N_e is related to the fraction of the primary energy converted to neutral pions, the number of muons at ground level is closely connected to the energy fraction transformed into charged pions and the mean free path between secondary hadron interactions. Hence N_μ also provides a primary dependent measure of E_0. N_μ as a function of E_0 is plotted in figure 10a for hydrogen, oxygen and iron nuclei initiated showers. The dependence of N_μ on E_0 can be described by:

$$N_\mu = G \cdot E_0^g \tag{6}$$

which is analogous to equations 2 and 4 (see sections 4.1 and 4.2). The number of muons in a shower is much smaller than both the number of electrons and the number of Cherenkov photons. Therefore, the minimum primary energy required for the application of any method using muons is higher in practice (around 1 PeV) than that necessary to the methods based on N_e or on the Cherenkov light. At a given E_0 value, the dependence of N_μ on A is a consequence of the dependence of f_{em} on A. A knowledge of ρ_{hump} thus allows one to correct N_μ, turning the corrected parameter N_μ^c into a primary independent measure of E_0. A correction has been considered of the form:

$$N_\mu^c = N_\mu \times (\rho_{hump} \cdot \mathrm{m}^2)^\gamma \qquad (7)$$

where γ is a free parameter which has been chosen so that the function $N_\mu^c(E_0)$ becomes primary independent. The effect of such a correction is illustrated in figure 10b for the sample of 10 degree zenith angle events. A light density dependent γ parameter, ranging from 1 to 2 and analogous to β in section 4.2, has been applied. This parameter minimizes the dependence on A across the whole energy interval. By means of a procedure similar to that described in sections 4.1 and 4.2, the error expected in the E_0 determination has been calculated for an ideal detector. An error of 11% (3%) for proton (iron) initiated showers has been obtained in the energy range above 500 TeV, where measurement of N_μ is feasible. This error is significantly lower than those achieved via the N_e and ρ_{hump} methods.

5 Conclusions

Three different methods for the energy measurement of extensive air showers initiated by cosmic rays in the energy range 10^{13} - 10^{16} eV have been introduced. The shower size is related to the EM energy of the shower and therefore can only provide an accurate measure of E_0 if the nature of the primary particle is known. The Cherenkov light density at the hump in the lateral distribution (and beyond the hump) is a better measure of the EM energy.

It has been demonstrated that both f_{em} and X_{max} depend on the primary energy per nucleon in similar ways and therefore X_{max} allows an estimate of the expected f_{em} value independent of the primary type. Since X_{max} can be determined from the slope of the Cherenkov lateral distribution, a correction can be applied to N_e or ρ_{hump} in such a way that the corrected parameter becomes a primary independent measure of E_0. Since for a fixed primary energy f_{em} and X_{max} are uncorrelated, the f_{em} fluctuations limit the effectiveness of such a correction. The influence of statistical fluctuations in the shower is reduced in the case of the N_e correction, but the reverse is true for the Cherenkov light correction. Neglecting detector effects, errors in the primary independent measurement of E_0 have been found to range from 19% (below 100 TeV) to 12% (above 500 TeV) for proton, from 16% to 6% for oxygen and from 30% to 6% for iron initiated showers. These values are slightly higher when using the method based on the Cherenkov light. The primary energy of γ-ray showers can be very accurately determined via the Cherenkov light measurement (5% uncertainty).

An array of Cherenkov light counters is essential in order to apply both methods. Our MC simulations predict that a higher accuracy in the measurement of E_0 can be obtained from the light beyond the hump (taking ρ_{200} for instance). In practice, the measurement of ρ_{200} faces two major obstacles: the finite size of the array may be insufficient to cover the light disc and signal is degraded by the night sky background light. An array of electron counters is an additional requirement when applying the method based on the shower size. These methods are currently being applied in the HEGRA experiment, for which a precise detector simulation shows that both methods are practicable [18].

Lastly, a method based on the simultaneous measurement of the number of muons and ρ_{hump} has been described, which has proven to be very precise (about 15% error) at high energies (E>500 TeV).

All of these results hold under the approximations of our Monte Carlo code (CORSIKA). In a recent comparison with other MC approaches [17], discrepancies in X_{max} for extreme models were found to be below 20 g/cm^2 for all primary nuclei. The most extreme differences in N_e and N_μ for proton (Fe) showers were of the order of 35% (15%) at 10^{14} eV and 40% (30%) at 10^{15} eV. A comparison of the Cherenkov light yields from the various models has not yet been carried out. The effect of the different models upon those correlations between shower observables which form the basis of our methods is still unknown.

These methods allow one to measure the energy of a primary cosmic ray when the nature of the particle is not known. Hence, they enable existing detectors, such as HEGRA (where they are now being applied) to measure the cosmic ray all-particle energy spectrum in a way which is independent of the (still unknown) chemical composition at energies near the knee.

6 Acknowledgments

We greatly appreciated the discussions with M. Rozanska and our colleagues in the HEGRA collaboration, especially A. Lindner in Hamburg and B. Wiebel in Wuppertal, who are presently carrying out similar studies, using somewhat different approaches. This work would have been impossible without the support of our colleagues in the HEGRA Madrid group and the use of its facilities. We would like to express our appreciation to the authors of CORSIKA for providing us with their simulation code and especially to Dr. Heck and Dr. Knapp for their valuable assistance. We are also indebted to S.M. Bradbury for corrections to the manuscript. This work has been supported by the Spanish Research Council CYCIT.

References

[1] Hillas A M 1983 Proc. Cosmic Ray Workshop, Uni. of Utah 16.
Hillas A M 1984 Annu. Rev. Astron. Astrophys. **22** 425.

[2] Kalmykov N N and Khristiansen G B 1995 J. Phys. G **21** 1279.

[3] Rhode W et al 1996 Nuclear Physics B (Proc Suppl) **48** 491-493.

[4] Nagano M et al 1984 J. Phys. G **10** 1295.
Gibbs K G 1988 Nucl. Instrum. Methods A **264** 67.
Alexandreas D E et al 1992 Nucl. Instrum. Methods A **311** 350.
Vildanova L I et al 1994 Izv. RAN Ser. Phys. **58** 79.
Amenomori M et al 1996 Ap. J. **461** 408.

[5] Klages H O 1997 Nucl. Phys. **52B** 92.

[6] Thornton G and Clay R 1981 Phys. Rev. D **43** 2090.
Linsley J and Watson A A 1981 Phys. Rev. Lett. **46** 459.
Stanev T et al 1983 Proc. 18th Int. Cosmic Ray Conf. (Bangalore) **2** 111.
Battistoni G et al 1985 Proc. 19th Int. Cosmic Ray Conf. (La Jolla) **2** 158.
Mincer A I et al 1985 Proc. 19th Int. Cosmic Ray Conf. (La Jolla) **3** (1985) 201.
Degrange B 1985 Proc. 19th Int. Cosmic Ray Conf. (La Jolla) **8** 1.

[7] Sokolsky P 1989 Introduction to Ultrahigh Energy Cosmic Ray Physics ed Addison Wesley (Redwood City, CA).

[8] Karle K et al 1993 Proc. 23rd Int. Cosmic Ray Conf. (Calgary) **4** 666.
Karle K et al 1995 Astrop. Phys. **3** 321.

[9] Lindner A 1996 Proc. XVth Cracow Summer School of Cosmology.

[10] Patterson J R and Hillas A M 1983 J. Phys. G **9** 1433.

[11] Cronin J W, Gibbs K G and Weekes T C 1993 Annu. Rev. Nucl. Part. Sci. **43** 883.
Lorenz E 1996 Nucl. Phys. B (Proc. Suppl.) **48** 391.

[12] Martinez S et al 567 1995 Nucl. Instrum. Meth. A **357** 567.
Martinez S 1996 Ph.D. thesis, Univ. Complutense Madrid.

[13] Capdevielle J N et al 1993 KfK Report 4998.
Knapp J and Heck D 1994 KfK Report 5196B.

[14] Nelson W R et al 1995 SLAC Report 265.

[15] Fesefeldt H 1985 The Simulation of Hadron Showers, RWTH Aachen Report PITHA 85/02.

[16] Werner W 1993 Physics Reports **232** 87.

[17] Knapp J et al 1996 KfK Report FZKA 5828.

[18] Cortina J, PhD thesis (in preparation).

[19] Boley F I 1964 Rev. Mod. Phys. **36** 792.
Jelley J V 1967 Progr. in Element. Part. and Cosmic Ray Phys. **9** 41.

Hillas A M 1982 J. Phys. G **8** 1461.
Rao M V S and Sinha S 1988 J. Phys. G **14** 811.
Turver K E. 1992 Nucl. Phys. B (Proc. Suppl) **28B** 16.

[20] Gabriel T A et al 1994 Nucl. Instrum. Meth. A **A338** 336.
Arqueros F et al 1996 Astropart. Phys. **4** 309.

[21] Bott-Bodenhausen M et al 1992 Nucl. Instrum. Meth. A **315** 236.

Figure captions

Fig. 1 Shower maximum depth versus primary energy for cosmic ray showers of 10° zenith angle. For each primary, the dashed line represents the mean value of X_{max} while the shaded region contains the fluctuations (root mean square). The upper region corresponds to protons, the middle region to oxygen nuclei and the lower region to iron nuclei.

Fig. 2 Fraction of the energy transferred to the electromagnetic channel (before reaching an observation level of 800 g/cm^2) versus a) the total primary energy and b) the primary energy per nucleon, for 10° showers initiated by protons (filled circles), oxygen nuclei (open circles) and iron nuclei (stars).

Fig. 3 Fraction of the energy transferred to the electromagnetic channel versus the shower maximum depth for those events of figure 2. The relationship between X_{max} and f_{em} is a consequence of the dependence of both parameters on the primary energy E_0. For a fixed E_0 value, X_max and f_em are uncorrelated.

Fig. 4 Relationship between the depth of the shower maximum and the light radius for 10° showers initiated by protons (filled circles), oxygen nuclei (open circles) and iron nuclei (stars).

Fig. 5 a) Shower size and b) corrected shower size as a function of the primary energy for 10° γ-ray (triangles), proton (filled circles) and iron (stars) induced showers. Symbols indicate the mean value of the (corrected) shower size for those events in the corresponding energy bin while vertical bars represent the root mean square of the distributions. N_e^c provides a primary independent measure of E_0 but has no physical meaning (see text).

Fig. 6 a) Shower size and b) Cherenkov light density at the hump as a function of the position of the shower maximum for 100 TeV proton (filled circles), oxygen (open circles) and iron (stars) induced showers. The zenith angle is 10°.

Fig. 7 Electromagnetic energy of hadronic showers as a function of a) the light density at the hump position and b) the light density at $\sim$ 200 m core distance, for protons (filled circles), oxygen nuclei (open circles) and iron nuclei (stars). The zenith angle is 10° and primary energy ranges from 10 TeV to 10 PeV.

Fig. 8 Number of Cherenkov photons arriving at a core distance r, generated in various atmospheric layers divided by the total number of photons generated in the layer $R_l(r)$. The ratios are normalized to the integral of the function $R_l(r)$. This figure corresponds to a γ-ray shower of 100 TeV and depths of

(a) 100-150 g/cm^2, (b) 300-350 g/cm^2, (c) 500-550 g/cm^2 and (d) 700-750 g/cm^2.

Fig. 9 a) Cherenkov light density and b) corrected Cherenkov light density at the hump, both as a function of the primary energy. The symbols indicate the mean for γ-rays (triangles), protons (filled circles), oxygen nuclei (open circles) and iron nuclei (stars). The zenith angle is 10°. Bars represent the σ of the Cherenkov light distributions for each energy bin. ρ^c_{hump} provides a primary independent measure of E_0 but has no physical meaning (see text).

Fig. 10 a) number of muons and b) corrected number of muons, both as a function of the primary energy. The symbols indicate the mean for protons (filled circles), oxygen (open circles) and iron (stars). The zenith angle is 10°. Bars represent the σ of the distribution of the number of muons for each energy bin. N^c_μ provides a primary independent measure of E_0 but has no physical meaning (see text).

Table captions

Tab. 1 Percentage errors (root mean square) in the E_0 determination from the shower size (Δ_p) and from parameter N_e^c, in the event that the primary type is ignored (Δ_i^c) or known (Δ_p^c). The zenith angle is 10°. We have estimated the absolute errors of the percentage uncertainties in E_0 due to our limited statistics. These errors typically range from ± 2 to ± 5, increasing with E_0, because the number of simulated events is much smaller at higher energies.

Tab. 2 Percentage errors (root mean square) in the E_0 determination from the Cherenkov light density at the *hump* (Δ_{hump}), from the parameter ρ^c_{hump} (Δ^c_{hump}) and from the parameter ρ^c_{200} (Δ^c_{200}) always for a primary independent correction. The zenith angle is 10°. The absolute errors in the percentage uncertainties due to our limited statistics are typically about ± 2.

Tables

	Δ_p			Δ_i^c			Δ_p^c		
	E_0 range (TeV)								
Primary	<100	100-500	>500	<100	100-500	>500	<100	100-500	>500
γ	31	27	-	-	-	-	15	15	-
p	41	32	22	19	16	12	19	15	12
O	27	15	15	16	11	6	12	9	6
Fe	16	15	7	30	15	6	16	12	6

Table 1:

	Δ_{hump}			Δ_{hump}^c			Δ_{200}^c		
	E_0 range (TeV)								
Primary	<100	100-500	>500	<100	100-500	>500	<100	100-500	>500
γ	9	5	5	-	-	-	-	-	-
p	24	18	17	46	36	26	37	28	27
O	10	8	4	42	14	12	20	12	10
Fe	8	6	4	36	17	6	22	12	6

Table 2:

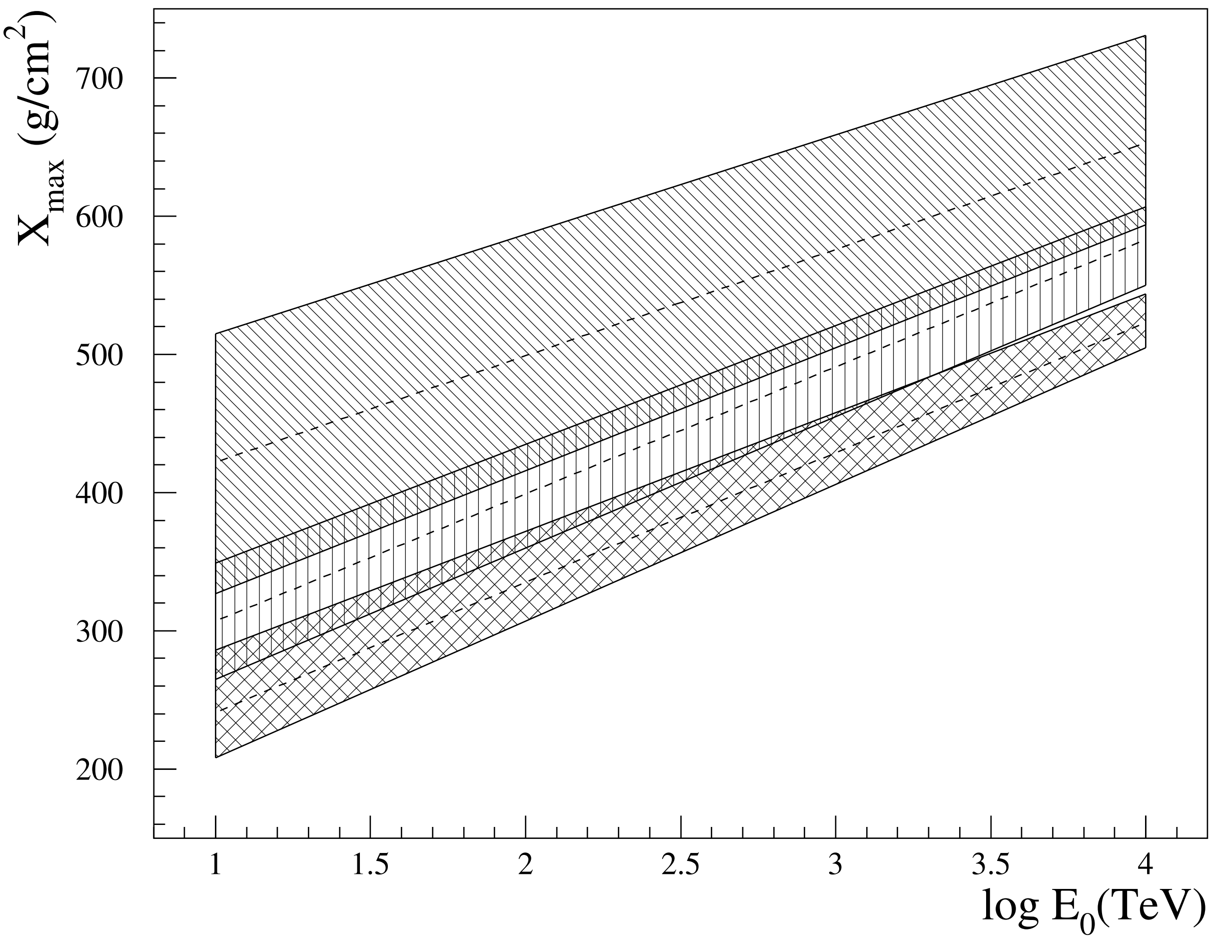

Figure 1:

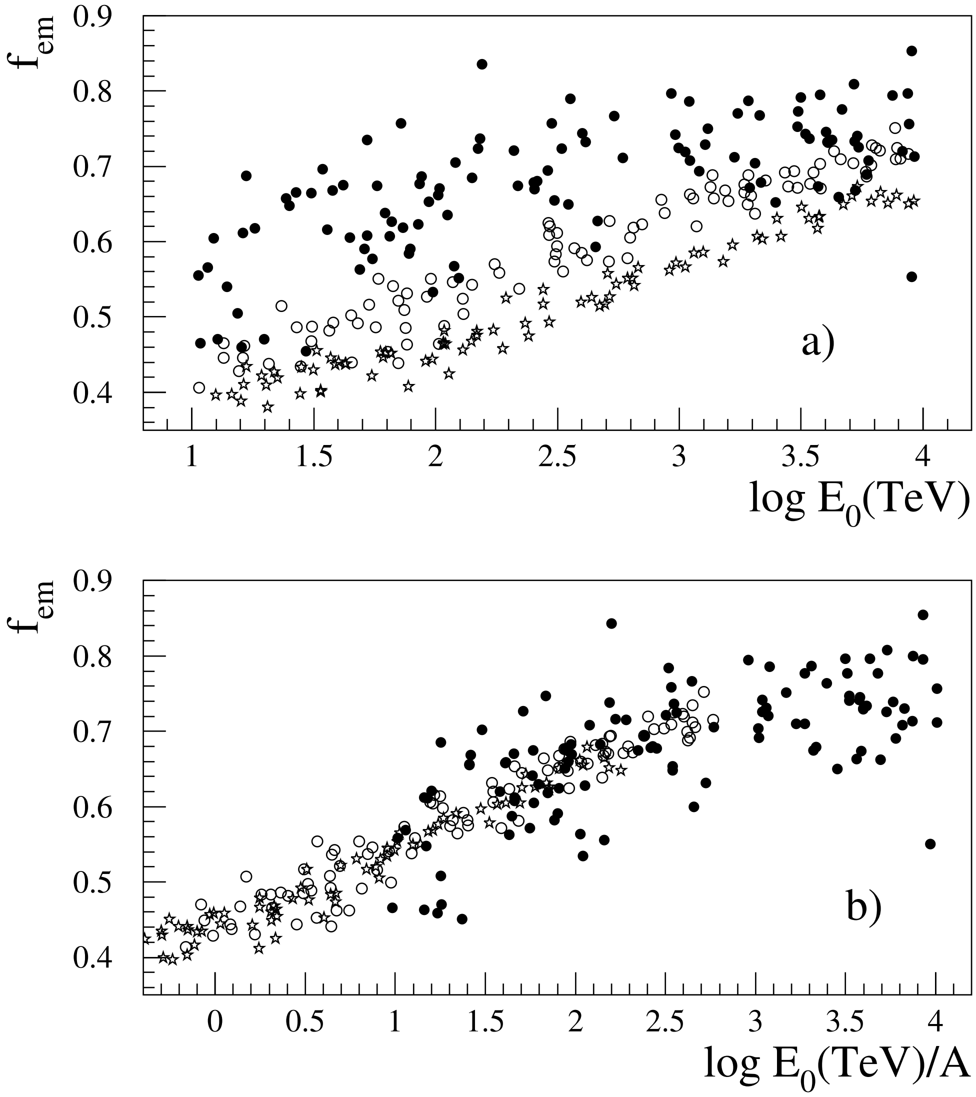

f_em
0.9
0.8
0.7
0.6
0.5
0.4
a)
1
1.5
2
2.5
3
3.5
4
log E_0(TeV)
f_em
0.9
0.8
0.7
0.6
0.5
0.4
b)
0
0.5
1
1.5
2
2.5
3
3.5
4
log E_0(TeV)/A

Figure 2:

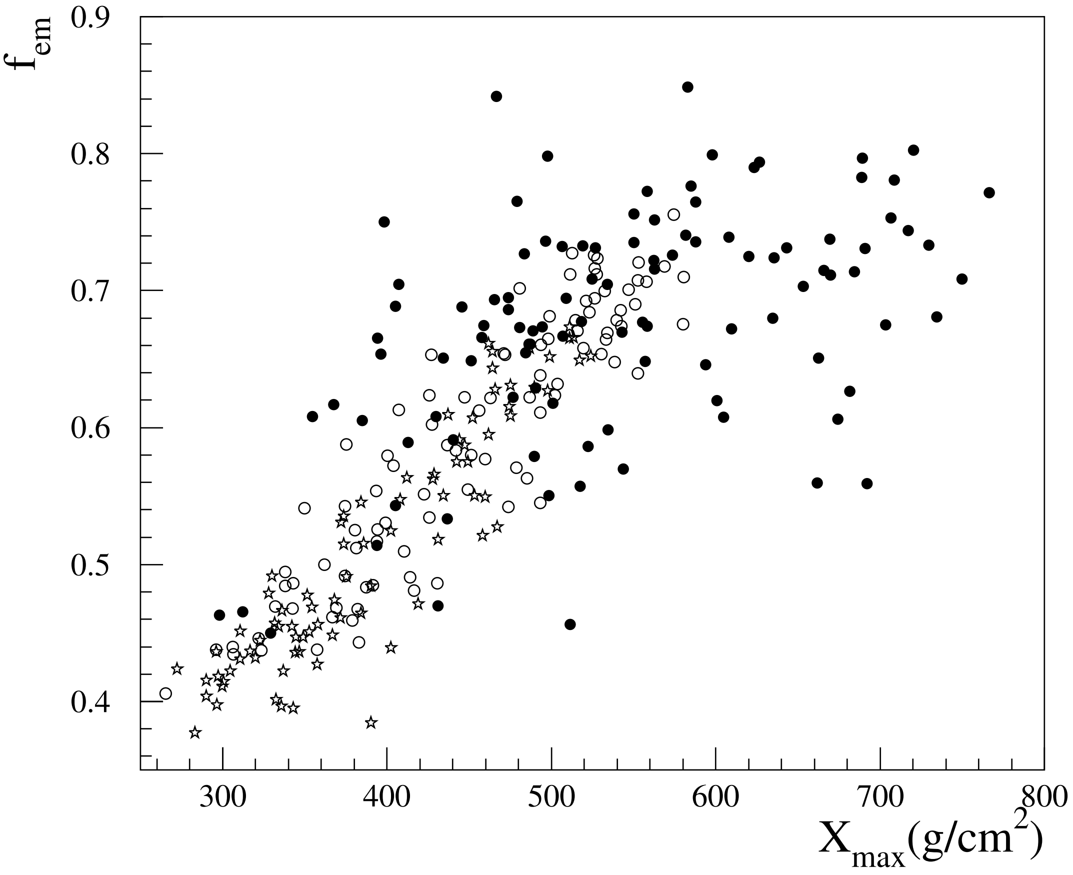

Figure 3:

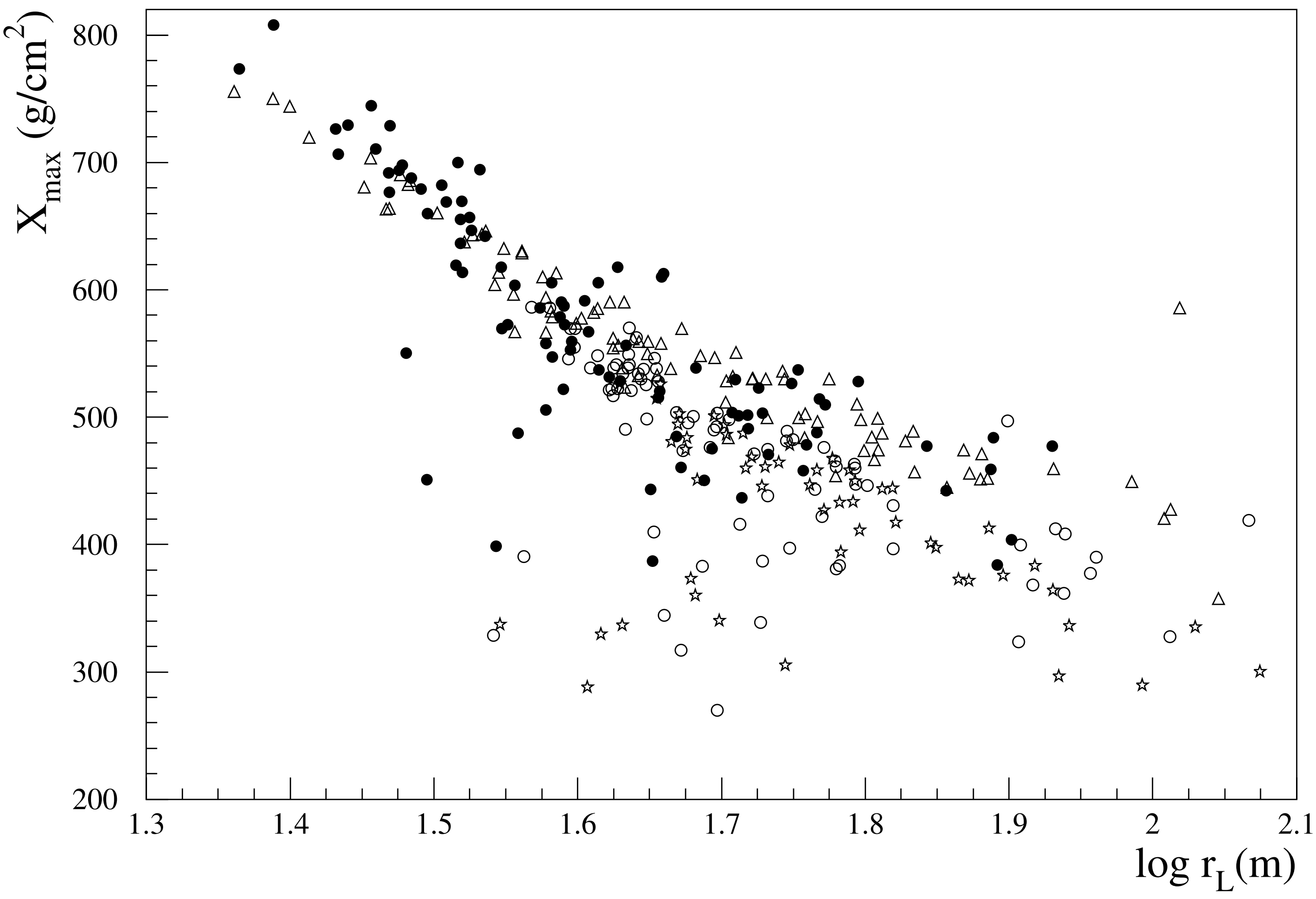

X_max (g/cm^2)
800
700
600
500
400
300
200
1.3
1.4
1.5
1.6
1.7
1.8
1.9
2
2.1
log r_L(m)

Figure 4:

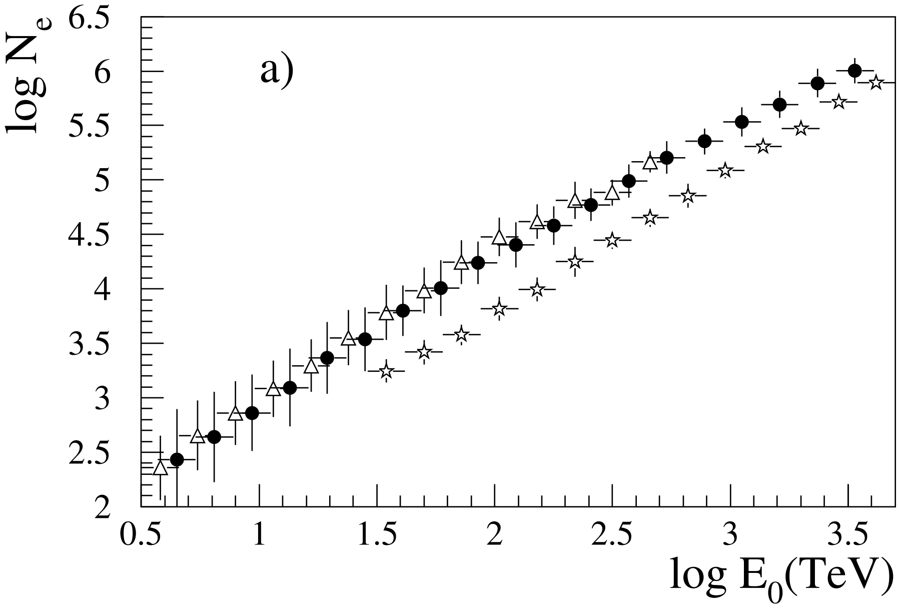
a)
log N_e
log E_0(TeV)
0.5
1
1.5
2
2.5
3
3.5
2
2.5
3
3.5
4
4.5
5
5.5
6
6.5

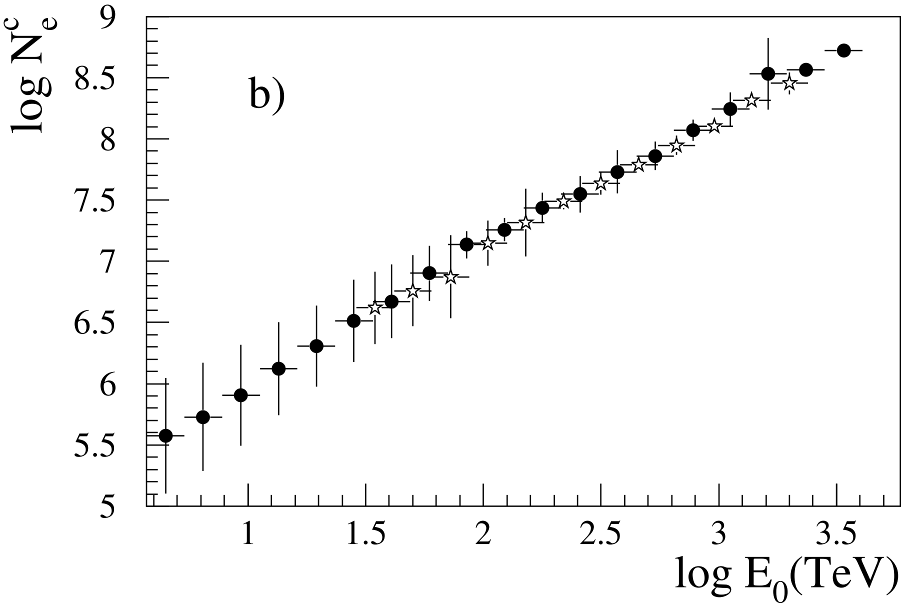
b)
log N_e^c
log E_0(TeV)
1
1.5
2
2.5
3
3.5
5
5.5
6
6.5
7
7.5
8
8.5
9

Figure 5:

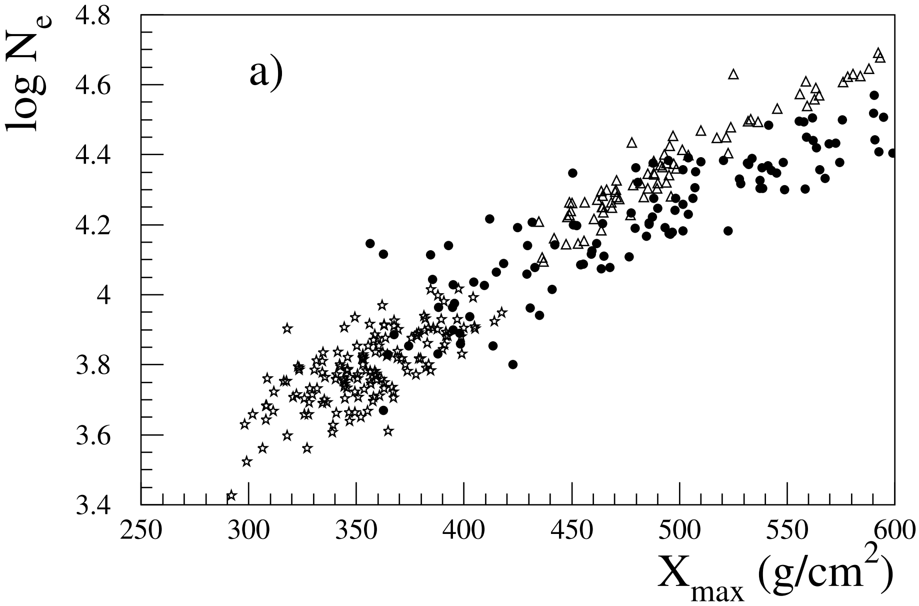

log N_e
a)
4.8
4.6
4.4
4.2
4
3.8
3.6
3.4
250
300
350
400
450
500
550
600
X_max (g/cm^2)

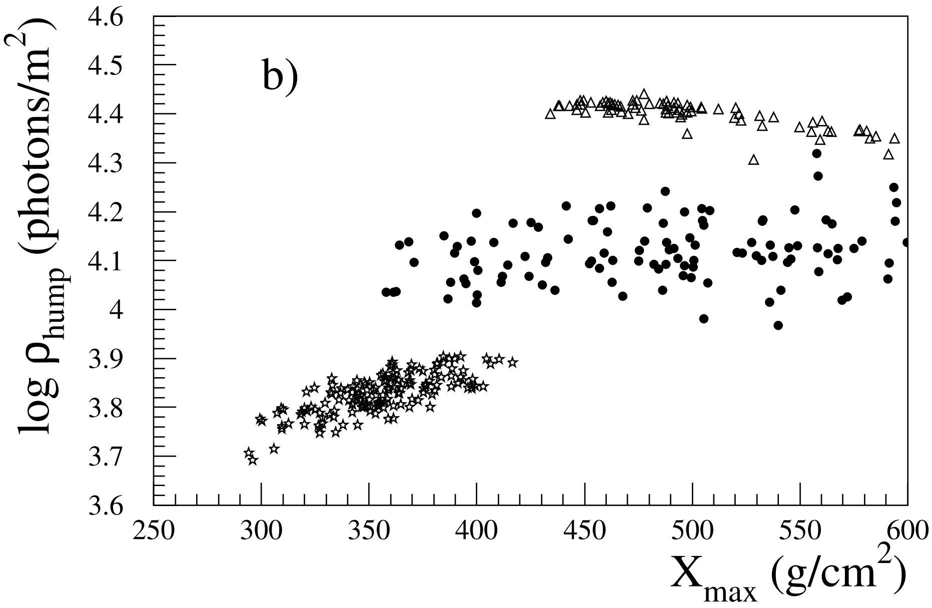

log ρ_hump (photons/m^2)
b)
4.6
4.5
4.4
4.3
4.2
4.1
4
3.9
3.8
3.7
3.6
250
300
350
400
450
500
550
600
X_max (g/cm^2)

Figure 6:

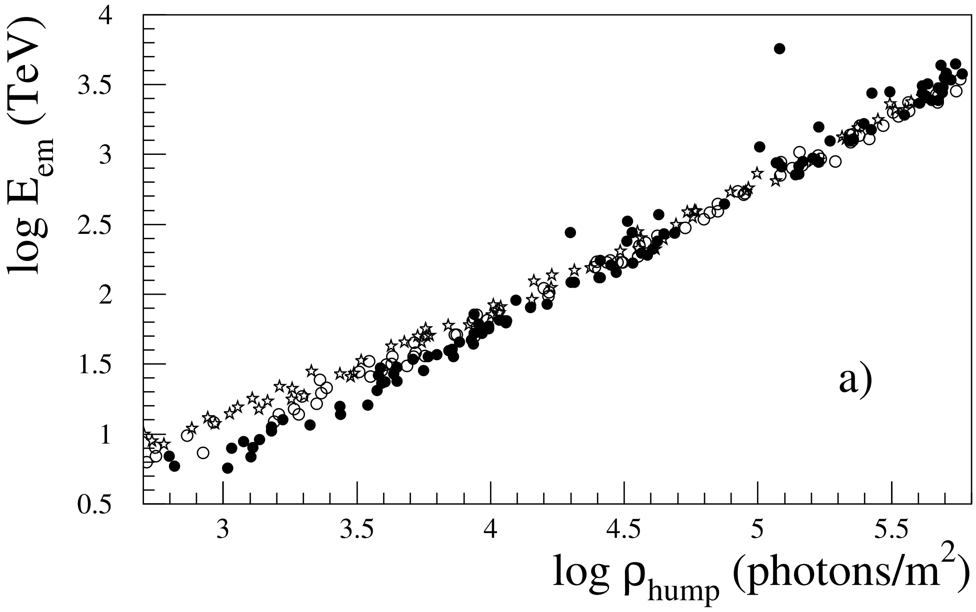

log E$_{em}$ (TeV)
4
3.5
3
2.5
2
1.5
1
0.5
3
3.5
4
4.5
5
5.5
a)
log ρ_{hump} (photons/m^2)

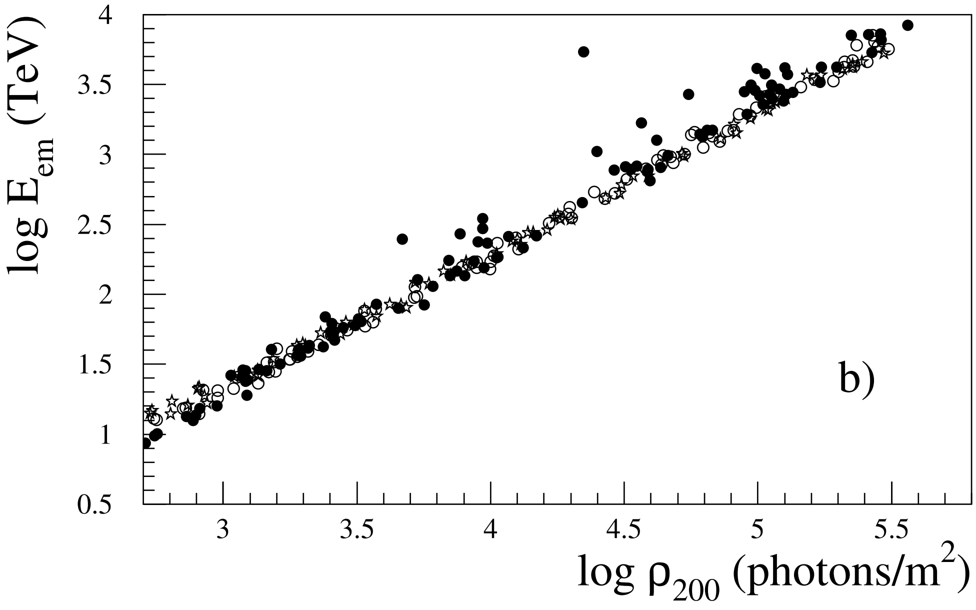

log E$_{em}$ (TeV)
4
3.5
3
2.5
2
1.5
1
0.5
3
3.5
4
4.5
5
5.5
b)
log ρ_{200} (photons/m^2)

Figure 7:

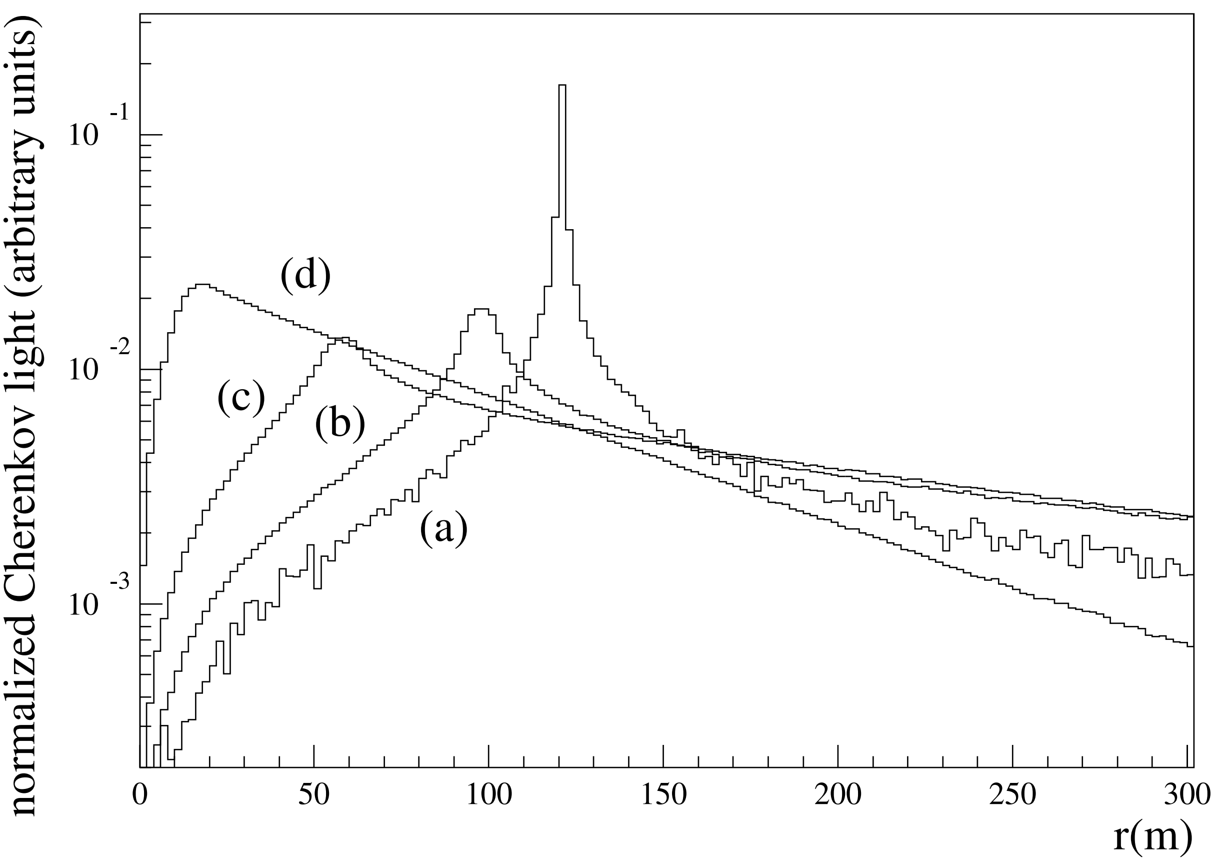
normalized Cherenkov light (arbitrary units)
10 -1
10 -2
10 -3
(d)
(c)
(b)
(a)
0
50
100
150
200
250
300
r(m)

Figure 8:

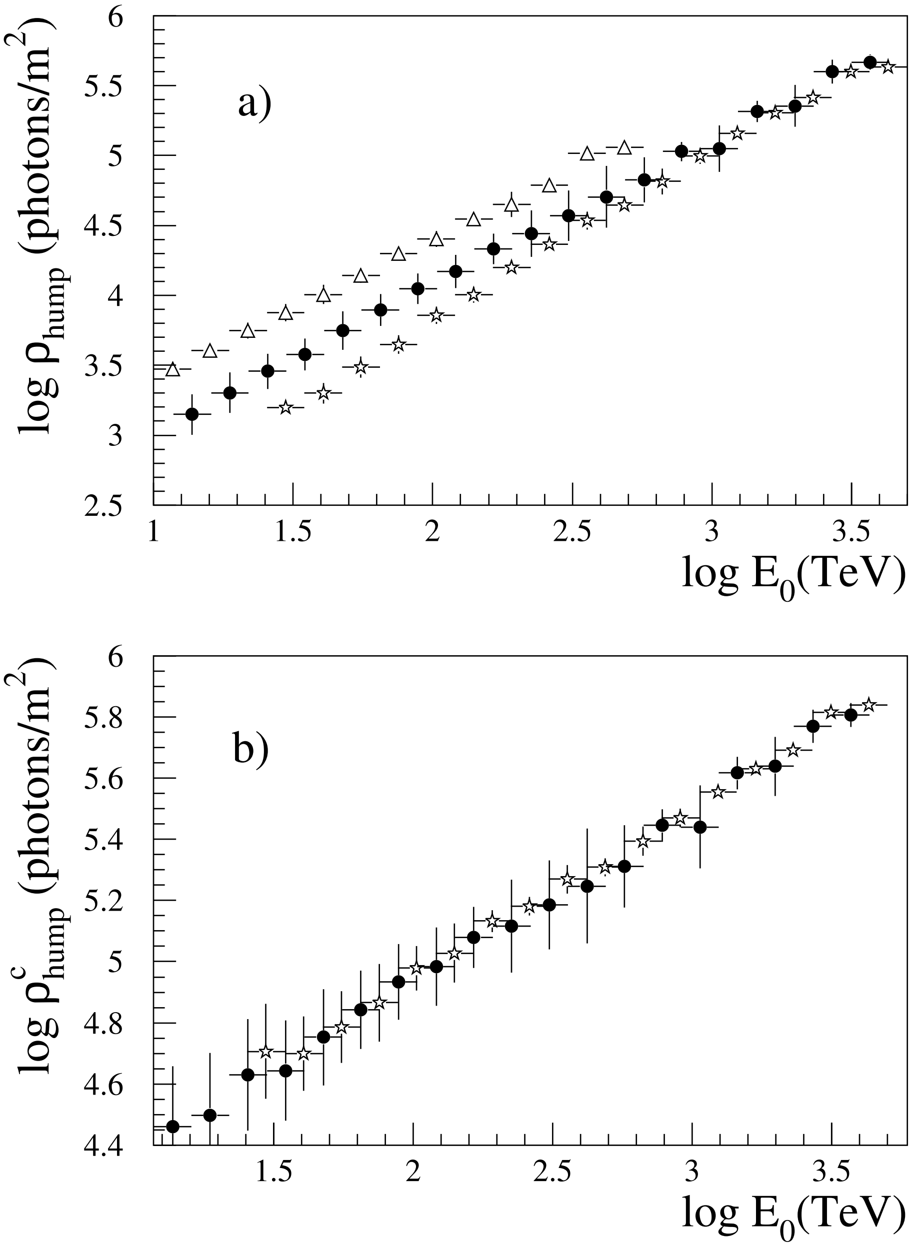
a)
log ρhump (photons/m2)
log E0(TeV)
b)
log ρchump (photons/m2)
log E0(TeV)

Figure 9:

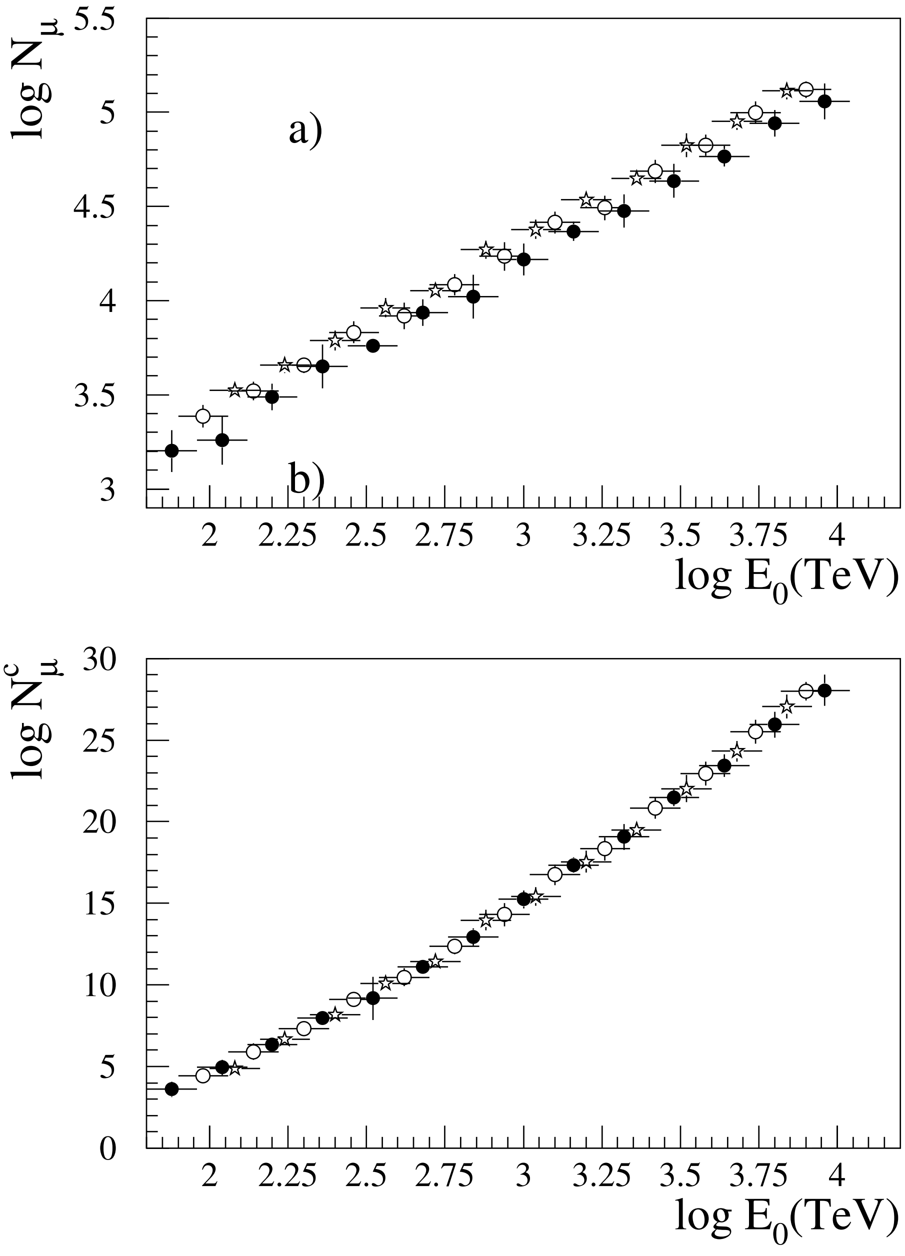

Figure 10: